

The covering factor of high redshift damped Lyman- α systems

N. Kanekar^{1*}, W. M. Lane², E. Momjian¹, F. H. Briggs³, J. N. Chengalur⁴

¹*National Radio Astronomy Observatory, 1003 Lopezville Rd, Socorro, NM 87801, USA;*

²*Naval Research Laboratory, Code 7213, 4555 Overlook Ave SW, Washington, DC 20375, USA*

³*Australian National University, ACT 2611, Australia*

⁴*National Centre for Radio Astrophysics, Ganeshkhind, Pune-411007, India*

Received mmdyy/ accepted mmdyy

ABSTRACT

We have used the Very Long Baseline Array to image 18 quasars with foreground damped Lyman- α systems (DLAs) at 327, 610 or 1420 MHz, to measure the covering factor f of each DLA at or near its redshifted H I 21cm line frequency. Including six systems from the literature, we find that none of 24 DLAs at $0.09 < z < 3.45$ has an exceptionally low covering factor, with $f \sim 0.45 - 1$ for the 14 DLAs at $z > 1.5$, $f \sim 0.41 - 1$ for the 10 systems at $z < 1$, and consistent covering factor distributions in the two sub-samples. The observed paucity of detections of H I 21cm absorption in high- z DLAs thus cannot be explained by low covering factors and is instead likely to arise due to a larger fraction of warm H I in these absorbers.

Key words: quasars: individual : quasars: images– galaxies: ISM

1 INTRODUCTION

Damped Lyman- α systems (DLAs), selected on the basis of their high H I column densities ($N_{\text{HI}} \geq 2 \times 10^{20} \text{ cm}^{-2}$) in quasar absorption spectra, have long been identified as the progenitors of normal present-day galaxies (Wolfe et al. 1986), and have hence been the subject of much research. Despite this, the nature of high- z DLAs, physical conditions in them, and their evolution with redshift, are still matters of dispute today (e.g. Wolfe et al. 2005). An issue of recent controversy is the temperature distribution of H I in DLAs. For radio-loud background quasars, a comparison between the H I column density and the optical depth in the redshifted H I 21cm line yields the DLA spin temperature (T_s). For optically-thin multi-phase absorption, T_s is the column-density-weighted harmonic mean of the spin temperatures of the different phases along the line of sight. For nearly three decades, the spin temperatures of high- z DLAs have been found to be systematically higher than values seen in the Milky Way or local spiral disks (e.g. Wolfe & Davis 1979; Carilli et al. 1996; Kanekar & Chengalur 2003); the first low- T_s DLA at high redshift was only detected very recently (York et al. 2007). The simplest interpretation of the observations is that H I in high- z DLAs is predominantly warm, unlike the situation in the Galaxy (Carilli et al. 1996; Chengalur & Kanekar 2000; Kanekar & Chengalur 2003). Conversely, Wolfe et al. (2003) used CH* absorption lines to argue that roughly half the DLAs at $z \gtrsim 2$ contain significant fractions of cold H I.

A problem in measuring DLA spin temperatures is that low-frequency radio emission is often extended over large angular scales, far larger than the size of a galaxy. Redshifted H I 21cm absorption studies are usually carried out with single dishes or short-

baseline interferometers, of fairly poor angular resolution, $\gtrsim 10''$, or $\gtrsim 80 \text{ kpc}$ at $z \sim 3$. It is hence often not certain that the quasar radio emission is entirely covered by the foreground DLA. If some fraction of the quasar emission leaks out around the DLA, the inferred spin temperature will be an over-estimate. The fraction of the radio emission occulted by the DLA is referred to as the covering factor f (e.g. Briggs & Wolfe 1983).

Recently, Curran et al. (2005) have emphasized the problem of unknown covering factors in high- z DLAs, pointing out that the high estimated T_s values of Kanekar & Chengalur (2003) (hereafter KC03) could merely stem from very low DLA covering factors, $f \ll 1$. Curran & Webb (2006) also argued that low DLA covering factors at high redshifts arise due to a geometrical effect, as the similarity in angular diameter distances of the high- z DLAs and their background quasars implies that a high- z DLA is “less effective” at covering the quasar than a low- z absorber. Note that Curran et al. (2005) find that quasars of angular extent $\lesssim 0.1''$ are adequately covered even by compact foreground DLAs.

The most direct way of resolving this issue is by high spatial resolution very long baseline interferometry (VLBI) studies in the redshifted H I 21cm line (e.g. Briggs et al. 1989; Lane et al. 2000). Unfortunately, the low-frequency coverage of current VLBI facilities is quite limited, implying that such observations are only possible for very few sources. Alternatively, one could measure the compact flux density arising from the quasar core in VLBI continuum images at or near the redshifted H I 21cm line frequency and then estimate the DLA covering factor by comparing the VLBI flux density with the flux density measured with short baseline interferometers or single dishes (e.g. Briggs & Wolfe 1983; Kanekar et al. 2007). This is the approach that we follow here, based on Very Long Baseline Array (VLBA) imaging of 18 quasars with foreground DLAs at $z \sim 0.24 - 3.45$.

* E-mail: nkanekar@nrao.edu (NK)

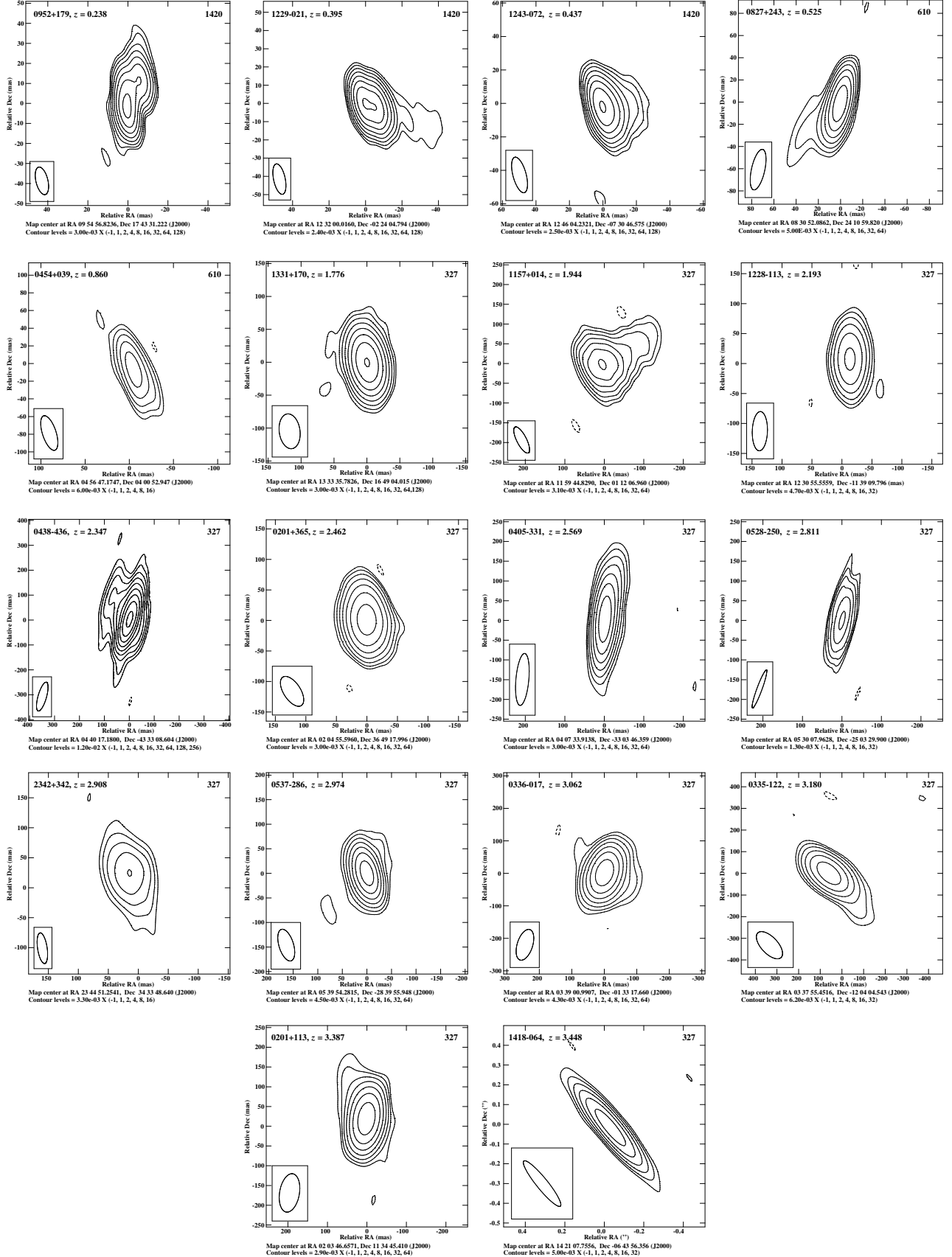


Figure 1. VLBA images of the 18 quasars of the sample, ordered (from top left) by DLA redshift. The map frequency is at the top right of each panel.

2 OBSERVATIONS, DATA ANALYSIS AND RESULTS

The VLBA 1.4 GHz, 610 MHz and 327 MHz receivers were used to observe the 18 quasars of our sample between 2002 March and 2006 June (projects BK89 and BK131), with observing frequencies close to the redshifted H α 21cm line frequency of the foreground DLA. Three quasars with DLAs at $z \sim 0.24 - 0.44$ were observed at 1.4 GHz, two, with DLAs at $z \sim 0.52 - 0.86$, at 610 MHz, and 13, with DLAs at $z \sim 1.78 - 3.45$, at 327 MHz. Total bandwidths of 4, 8 and 16 MHz were used for the observations at 610 MHz, 327 MHz and 1420 MHz, respectively, with 2-bit sampling, two polarizations, 16 spectral channels and on-source integration times of 1 – 4 hours. Strong fringe finders (3C345, 3C454.3 or 3C286) were observed every few hours, to calibrate the shape of the pass-band. Phase-referencing was not used. The U-V coverage was poor in some cases, as all the VLBA antennas were not available, resulting in asymmetric or larger synthesized beams.

The data were analysed in “classic” AIPS, using standard techniques. Initial procedures included ionospheric corrections, editing of radio frequency interference, amplitude calibration (using the measured antenna gains and system temperatures), pass-band calibration and fringe-fitting for the delay rates, before the data for each target were averaged in frequency to a single-channel dataset. For each source, this was followed by a number of cycles of self-calibration and imaging to determine the antenna gains, until no improvement was seen on further self-calibration. The final images obtained from the above procedure are shown in Fig. 1, in order of increasing redshift, with the synthesized beams listed in column (6) of Table 1. The root-mean-square noise in off-source regions in the images was measured to be $\sim 0.5 - 3$ mJy/Bm.

The task UVFIT was used to fit elliptical gaussian models to the visibility data, to measure the compact flux density. Most sources in Fig. 1 are core-dominated, with only a small fraction of the flux density in extended structure. For some sources with visible extensions (e.g. 1229–021, 1243–072 and 0201+113), a single-component model was found sufficient to recover the “cleaned” flux density. The only exceptions are 0952+179 ($z_{\text{abs}} \sim 0.238$), 1157+014 ($z_{\text{abs}} \sim 1.944$) and 0438–436 ($z_{\text{abs}} \sim 2.347$), where all the “cleaned” flux density could be recovered only with a 2-component model.

Table 1 summarizes the results of the VLBA observations, grouping the sources by observing band, in order of increasing redshift. For each source, the first four columns contain the observing band, source name, DLA redshift and redshifted H α 21cm frequency. Column (5) lists the total flux densities at the VLBA observing frequency. For the three 1.4 GHz targets, this was obtained from the 1.4 GHz NRAO VLA Sky Survey (Condon et al. 1998). For most 327 MHz targets (11/13), we use the flux density measured at nearby frequencies [e.g. at 327 MHz, from the Westerbork Northern Sky Survey (Rengelink et al. 1997), 365 MHz, from the Texas survey (Douglas et al. 1996), Carilli et al. (1996) or KC03]. Four sources (0827+243, 0454+039, 0405–331 and 0438–436) do not have measurements in the literature near the VLBA observing frequencies; their flux densities were hence estimated from their low-frequency (< 1 GHz) spectral indices.

Columns (6 – 10) contain (6) the VLBA synthesized beam, (7) the flux density obtained on fitting a gaussian model with UVFIT, (8) the deconvolved angular sizes of the gaussian components, (9) the corresponding spatial extents of these components, at the redshift of the foreground DLA [we use $(\Omega_{\Lambda}, \Omega_m, h) = (0.7, 0.3, 0.7)$ in this paper] and (10) the covering factor of the compact radio emission at the observing frequency, obtained by divid-

ing the “core” flux density by the total flux density. In three cases of two source components, the one that is more compact is identified with the core. We emphasize that the deconvolved sizes listed in columns (8) and (9) are upper limits, due to the possibility of residual phase errors in the data (e.g. due to fluctuations on time scales shorter than the self-calibration interval). This is especially true for the 327 MHz and 610 MHz results.

3 OTHER SOURCES

A few other quasars with foreground DLAs have estimates of the covering factor from VLBI studies. These are discussed below.

(1) 0738+313 ($z_{\text{abs}} \sim 0.0912, 0.2212$): Lane et al. (2000) used 1302 MHz VLBA observations to estimate that the covering factor of the foreground DLAs is $f \sim 0.98$.

(2) 1127–145 ($z_{\text{abs}} \sim 0.3127$): Bondi et al. (1996) measured a flux density of ~ 5.0 Jy in their 1.6 GHz VLBI image, compared to a single-dish flux density of ~ 5.6 Jy. This gives $f \sim 0.89$.

(3) 0235+164 ($z_{\text{abs}} \sim 0.524$): Wolfe et al. (1978) used 931 MHz VLBI observations to show that the size of the quasar core is < 6 mas. More recently, Frey et al. (2000) found that the 1.6 GHz VLBI core flux density (with a sub-mas beam) is very similar to that measured simultaneously with a single dish. This implies $f \sim 1$.

(4) 3C286 ($z_{\text{abs}} \sim 0.692$): Wilkinson et al. (1979) used 609 MHz VLBI observations to find that 17.5 Jy of the 609 MHz flux density (~ 20 Jy) arises in the central 55 mas. This implies $f \gtrsim 0.9$.

(5) 0458-020 ($z_{\text{abs}} \sim 2.039$): Briggs et al. (1989) used 608 MHz VLBI observations to estimate that the compact quasar core contains ~ 1.15 Jy at the redshifted H α 21cm line frequency of ~ 467 MHz, with an additional ~ 1.3 Jy in two extended components, on scales of $\sim 0''.2 - 0''.5$ and $\sim 1 - 2''$. They found the H α 21cm optical depths measured in VLBI and single-dish studies to be in excellent agreement and used this to argue that the entire $2''$ radio emission is likely to be covered, i.e. $f \sim 1$.

There are four DLAs with searches for H α 21cm absorption where the core fraction in the background quasar is very small, implying a low covering factor ($f \lesssim 0.1$). These are at $z \sim 0.437$ towards 3C196, $z \sim 1.3911$ towards 0957+561A, $z \sim 1.4205$ towards 1354+258 and $z \sim 0.656$ towards 3C336. Boisse et al. (1998) noted that the optical and radio sightlines towards 3C196 are clearly different, due to which T_s cannot be estimated. Similarly, KC03 found very small core fractions in 0957+561A and 1354+258, and argued that covering factor uncertainties preclude an estimate of the spin temperature. Conversely, Curran et al. (2007) do quote a (low) spin temperature for the DLA towards 3C336. However, the quasar is strongly lobe-dominated with the lobes extended over ~ 190 kpc, and only a small fraction of the flux density arises from the core (Bridle et al. 1994). As in the case of 3C196, the difference between radio and optical sightlines implies that it is not possible to estimate T_s in this absorber.

4 DISCUSSION

For H α 21cm absorption studies of DLAs towards radio-loud quasars, the H α 21cm optical depth τ_{21} , H α column density N_{HI} (cm^{-2}) and spin temperature T_s (K) are related by the expression

$$N_{\text{HI}} = 1.823 \times 10^{18} \times (T_s/f) \int \tau_{21} dV, \quad (1)$$

where f is the covering factor of the foreground DLA and the H α 21cm line is assumed to be optically thin. For a DLA, where N_{HI}

| V _{obs} | QSO | z _{abs} | V _{21cm} MHz | S _{tot} Jy | Beam mas × mas | S _{fit} mJy | Angular size mas × mas | Spatial extent pc × pc | f |
|------------------|----------|------------------|--------------------------|------------------------|-------------------|-------------------------|----------------------------|-----------------------------|------|
| 1.4 | 0952+179 | 0.238 | 1147.5 | 1.16 | 14 × 6 | 762 ± 1 | (1.7 ± 0.1) × (13.9 ± 0.1) | (6.4 ± 0.1) × (52.2 ± 0.1) | 0.66 |
| | | | | | | 303 ± 1 | (4.5 ± 0.1) × (9.1 ± 0.1) | (17.1 ± 0.1) × (34.1 ± 0.1) | – |
| 1.4 | 1229–021 | 0.395 | 1018.2 | 1.65 | 17 × 6 | 689 ± 1 | (14.9 ± 0.1) × (2.5 ± 0.1) | (79.6 ± 0.1) × (13.1 ± 0.8) | 0.42 |
| 1.4 | 1243–072 | 0.437 | 988.6 | 0.55 | 22 × 8 | 483 ± 1 | (7.7 ± 0.1) × (6.9 ± 0.1) | (43.6 ± 0.2) × (39 ± 1) | 0.88 |
| 610 | 0827+243 | 0.525 | 931.6 | 0.90 | 38 × 13 | 626 ± 6 | (2.3 ± 0.4) × (11.3 ± 0.4) | (16 ± 2) × (71 ± 3) | 0.70 |
| 610 | 0454+039 | 0.860 | 763.8 | 0.50 | 41 × 15 | 251 ± 9 | (31 ± 1) × (9 ± 1) | (241 ± 9) × (66 ± 9) | 0.50 |
| 327 | 1331+170 | 1.776 | 511.6 | 0.62 | 53 × 32 | 444 ± 5 | (26 ± 1) × (2 ± 2) | (223 ± 3) × (19 ± 14) | 0.72 |
| 327 | 1157+014 | 1.944 | 482.5 | 0.89 | 74 × 25 | 565 ± 15 | (39 ± 1) × (58 ± 1) | (327 ± 8) × (488 ± 9) | 0.63 |
| | | | | | | 132 ± 13 | (3 ± 35) × (107 ± 8) | (23 ± 297) × (897 ± 64) | – |
| 327 | 1228–113 | 2.193 | 444.8 | 0.51 | 65 × 25 | 290 ± 9 | (39 ± 2) × (24 ± 1) | (322 ± 18) × (196 ± 6) | 0.57 |
| 327 | 0438–436 | 2.347 | 424.4 | 7.64 | 120 × 34 | 4533 ± 15 | (19 ± 1) × (34 ± 1) | (156 ± 2) × (277 ± 2) | 0.59 |
| | | | | | | 1038 ± 18 | (123 ± 2) × (298 ± 12) | (1008 ± 11) × (2434 ± 101) | – |
| 327 | 0201+365 | 2.462 | 410.3 | 0.52 | 56 × 28 | 510 ± 6 | (10 ± 1) × (51.1 ± 0.4) | (79 ± 4) × (414 ± 3) | 0.98 |
| 327 | 0405–331 | 2.569 | 398.0 | 0.83 | 132 × 33 | 367 ± 5 | (7 ± 1) × (0 ± 2) | (55 ± 6) × (0 ± 15) | 0.44 |
| 327 | 0528–250 | 2.811 | 372.7 | 0.14 | 102 × 13 | 132 ± 5 | (49 ± 5) × (8 ± 3) | (384 ± 42) × (65 ± 20) | 0.94 |
| 327 | 2342+342 | 2.908 | 363.5 | 0.31 | 52 × 16 | 219 ± 10 | (49 ± 2) × (42 ± 2) | (372 ± 13) × (329 ± 12) | 0.71 |
| 327 | 0537–286 | 2.974 | 357.4 | 1.05 | 67 × 30 | 495 ± 4 | (10 ± 1) × (10 ± 1) | (77 ± 2) × (79 ± 10) | 0.47 |
| 327 | 0336–014 | 3.062 | 349.7 | 0.94 | 99 × 48 | 636 ± 7 | (37 ± 1) × (23 ± 2) | (286 ± 2) × (176 ± 18) | 0.68 |
| 327 | 0335–122 | 3.180 | 339.8 | 0.68 | 157 × 77 | 419 ± 8 | (31 ± 6) × (69 ± 2) | (233 ± 45) × (521 ± 11) | 0.62 |
| 327 | 0201+113 | 3.387 | 323.8 | 0.42 | 98 × 50 | 321 ± 8 | (21 ± 2) × (6 ± 4) | (152 ± 12) × (41 ± 28) | 0.76 |
| 327 | 1418–064 | 3.448 | 319.3 | 0.44 | 294 × 57 | 302 ± 11 | (23 ± 33) × (38 ± 2) | (167 ± 240) × (280 ± 11) | 0.69 |

Table 1. Results from VLBA low-frequency imaging of quasars behind high-*z* DLAs. See text for details and discussion.

is known from the Lyman- α profile, a measurement of the H_I 21cm optical depth hence yields (T_s/f) . Estimates of the covering factor can then be used to infer T_s for the DLA. High-*z* DLAs have long been found to have higher T_s values than seen in the Galaxy or local spirals (e.g. Wolfe & Davis 1979; Carilli et al. 1996; KC03). For example, KC03 found that all seven DLAs in their high-*z* sample had $T_s > 700$ K, while more than 80% of sightlines through the Milky Way and M31 have $T_s < 350$ K (Braun & Walterbos 1992). This suggests that high-*z* DLAs have far smaller fractions of the cold phase of H_I than local spirals (see also Carilli et al. 1996; Kanekar & Chengalur 2001). However, the T_s estimates depend on the estimated covering factors. If, as argued by Curran et al. (2005) and Curran & Webb (2006), high-*z* DLAs have systematically low covering factors, the high (T_s/f) measurements could arise due to low f values, and not due to high spin temperatures. Note that 5/7 high-*z* DLAs of the KC03 sample have $[T_s/f] \gtrsim 2000$ K; extremely low covering factors ($f < 0.2$) would then be needed to obtain spin temperatures in the “low” Galactic range ($T_s < 350$ K).

The covering factor of a DLA can be determined from VLBI studies at the redshifted H_I 21cm line frequency. Such studies are fairly common at frequencies $\gtrsim 1.4$ GHz, implying that it is usually straightforward to determine T_s for low-*z* DLAs ($z \lesssim 0.5$), for which the H_I 21cm line is redshifted to frequencies $\gtrsim 1$ GHz. However, for DLAs at $z \gtrsim 1.7$, the line frequency is redshifted to $\lesssim 500$ MHz, where it is technically difficult to carry out VLBI studies, as the coherent integration times are restricted by ionospheric fluctuations (Briggs 1983). This has meant that most T_s measurements in high-*z* DLAs are based on covering factors estimated either from VLBI studies at much higher frequencies (typically $\gtrsim 1.4$ GHz) or from the spectral index of the background quasar (e.g. Wolfe & Davis 1979; Wolfe et al. 1981; de Bruyn et al. 1996; Carilli et al. 1996; Kanekar & Chengalur 2003; Kanekar et al. 2006). Prior to this work, there were only three DLAs at $z \gtrsim 1.7$ with VLBI studies at $\lesssim 600$ MHz (Briggs & Wolfe 1983; Briggs et al. 1989), only one of which used more than two VLBI stations.

The full sample of quasars with DLA covering factor estimates from VLBI observations now consists of 24 systems, the 18 absorbers listed in Table 1 and six DLAs from the literature, discussed in the last section. We have excluded the four DLAs towards 3C196, 3C336, 0957+561A and 1345+258 (all at $z_{\text{abs}} < 1.5$), for which spin temperatures are not quoted in the literature due to their known low covering factors [except for 3C336; Curran et al. 2007]. The sample contains 14 DLAs at $z > 1.5$ and 10 at $z < 1.5$, the “high-*z*” and “low-*z*” sub-samples, respectively (the low-*z* DLAs are all at $z < 0.9$); the spatial extent of the core emission is $\lesssim 500$ pc at the DLA redshift in all cases except the $z \sim 2.039$ DLA towards 0458–020 (see below). No evidence for redshift evolution can be seen in Fig. 2[A], which plots the covering factor against redshift for the full sample. The median covering factor for the high-*z* sub-sample is $f_{\text{med}} \sim 0.685 \pm 0.042$, with $f \gtrsim 0.45$ for all high-*z* DLAs. The low-*z* sample has $f \sim 0.41 - 1$, with a median value of $f_{\text{med}} \sim 0.885 \pm 0.094$. A Kolmogorov–Smirnov rank-1 test yields a Gaussian probability of $\sim 72\%$ that the two sub-samples are drawn from different distributions, consistent (within $\sim 1.1\sigma$ significance) with the null hypothesis that they are drawn from the same distribution. Finally, the covering factors for the high-*z* sample were all determined at frequencies $\lesssim v_{21\text{cm}}$; these are hence *lower limits*, as the spectral index of core emission is usually inverted or flat, while extended non-thermal emission typically has a steep spectrum, and is hence fractionally larger at lower frequencies. This renders the difference between the low-*z* and high-*z* samples even less significant.

The deconvolved sizes of the “core” components are $\lesssim 70$ mas for all high-*z* DLAs in Table 1, corresponding to spatial sizes of $\lesssim 500$ pc at the DLA redshift. Fig. 2[B] shows the spatial extent of the “core” emission plotted against DLA redshift; for the sources of Table 1, fitted by an elliptical gaussian model, the “size” is the geometric mean of the deconvolved major and minor axes listed in Column (9) of the table. In all but one of the 24 systems, the size is $\lesssim 400$ pc, which would be entirely covered even by small (\gtrsim few kpc-sized) galaxies. The only exception is the $z \sim 2.039$

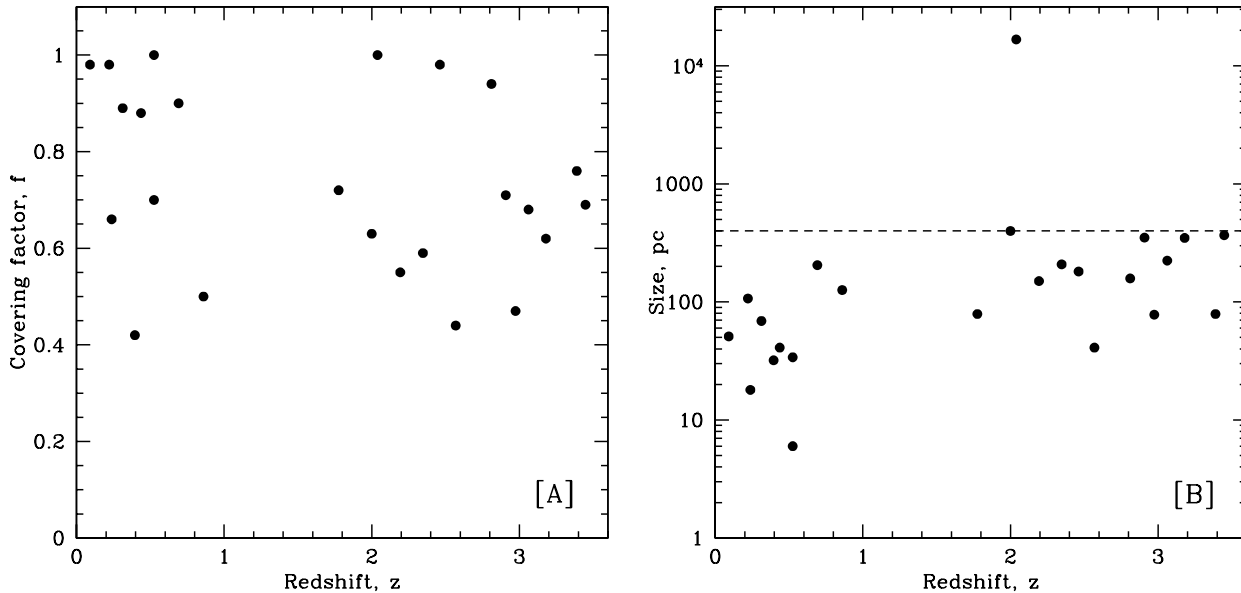


Figure 2. [A] Left panel: The covering factor of the 24 DLAs of the present VLBI sample, plotted against DLA redshift, z_{abs} . [B] Right panel: The spatial extent of the compact radio emission of the background quasars (at z_{abs}) plotted versus z_{abs} . The dashed line in [B] is at 400 pc. See text for discussion.

DLA towards 0458–020, where Briggs et al. (1989) find that the entire $\sim 2''$ radio emission is covered by the foreground DLA, implying an absorber size $\gtrsim 17$ kpc. Note that the larger deconvolved sizes typically obtained at high redshifts are at least partly due to the fact that all high- z DLAs were observed at 327 MHz, where residual phase errors in the data are likely to be an issue; as mentioned earlier, the deconvolved sizes should be treated as upper limits.

19 of the 24 systems plotted in Fig. 2 (of which ten are at $z > 1.5$) have T_s estimates in the literature [e.g. Wolfe & Davis 1979; Carilli et al. 1996; Kanekar et al. 2006; KC03]. It thus appears that the high T_s estimates in high- z DLAs are not the result of very low covering factors. The inferred high spin temperatures in high- z DLAs could then arise due to (1) a preponderance of warm HI in these systems (Carilli et al. 1996; KC03), or (2) systematically lower HI column densities on the radio sightlines than those measured towards the optical QSO, due to small-scale (sub-kpc) structure in the HI (Wolfe et al. 2003). The spatial resolution of the present VLBA data is not sufficient to rule out the possibility of differences between the optical and radio sightlines. However, good agreement (within a factor of ~ 2) has been found between HI column densities measured along the same sightline from Lyman- α absorption and low-resolution HI 21cm emission studies, both in the Galaxy (Dickey & Lockman 1990) and in the $z \sim 0.009$ DLA towards SBS 1549+593 (Chengalur & Kanekar 2002). This suggests that systematic large differences in HI column density between radio and optical sightlines in DLAs are unlikely. The high spin temperatures in high- z DLAs are thus more likely to be the result of a larger fraction of warm HI in these absorbers.

Acknowledgments

The National Radio Astronomy Observatory is operated by Associated Universities, Inc. under cooperative agreement with the National Science Foundation. NK acknowledges support from the Max Planck Foundation and an NRAO Jansky Fellowship, and thanks Craig Walker for discussions on the VLBA analysis. Basic Research in astronomy at the Naval Research Laboratory is supported by the Office of Naval Research.

REFERENCES

- Boisse P., Le Brun V., Bergeron J., Deharveng J.-M., 1998, *A&A*, 333, 841
- Bondi M., Padrielli L., Fanti R., Ficarra A., Gregorini L., Mantovani F., Bartel N., Romney J. D., Nicolson G. D., Weiler K. W., 1996, *A&A*, 308, 415
- Braun R., Walterbos R., 1992, *ApJ*, 386, 120
- Bridle A. H., Hough D. H., Lonsdale C. J., Burns J. O., Laing R. A., 1994, *AJ*, 108, 766
- Briggs F. H., 1983, *AJ*, 88, 239
- Briggs F. H., Wolfe A. M., 1983, *ApJ*, 268, 76
- Briggs F. H., Wolfe A. M., Liszt H. S., Davis M. M., Turner K. L., 1989, *ApJ*, 341, 650
- Carilli C. L., Lane W. M., de Bruyn A. G., Braun R., Miley G. K., 1996, *AJ*, 111, 1830
- Chengalur J. N., Kanekar N., 2000, *MNRAS*, 318, 303
- Chengalur J. N., Kanekar N., 2002, *A&A*, 388, 383
- Condon J. J., Cotton W. D., Greisen E. W., Yin Q. F., Perley R. A., Taylor G. B., Broderick J. J., 1998, *AJ*, 115, 1693
- Curran S. J., Murphy M. T., Pihlström Y. M., Webb J. K., Purcell C. R., 2005, *MNRAS*, 356, 1509
- Curran S. J., Tzanavaris P., Murphy M. T., Webb J. K., Pihlström Y. M., 2007, *MNRAS*, 381, L6
- Curran S. J., Webb J. K., 2006, *MNRAS*, 371, 356
- de Bruyn A. G., O’Dea C. P., Baum S. A., 1996, *A&A*, 305, 450
- Dickey J. M., Lockman F. J., 1990, *ARA&A*, 28, 215
- Douglas J. N., Bash F. N., Bozayan F. A., Torrence G. W., Wolfe C., 1996, *AJ*, 111, 1945
- Frey S., Gurvits L. I., Altschuler D. R., Davis M. M., Perillat P., Salter C. J., Aller H. D., Aller M. F., Hirabayashi H., 2000, *PASJ*, 52, 975
- Kanekar N., Chengalur J. N., 2001, *A&A*, 369, 42
- Kanekar N., Chengalur J. N., 2003, *A&A*, 399, 857
- Kanekar N., Chengalur J. N., Lane W. M., 2007, *MNRAS*, 375, 1528
- Kanekar N., Subrahmanyam R., Ellison S. L., Lane W. M., Chen-

- galur J. N., 2006, MNRAS, 370, L46
- Lane W. M., Briggs F. H., Smette A., 2000, ApJ, 532, 146
- Rengelink R. B., Tang Y., de Bruyn A. G., Miley G. K., Bremer M. N., Röttgering H. J. A., Bremer M. A. R., 1997, A&AS, 124, 259
- Wilkinson P. N., Readhead A. C. S., Anderson B., Purcell G. H., 1979, ApJ, 232, 365
- Wolfe A. M., Briggs F. H., Jauncey D. L., 1981, ApJ, 248, 460
- Wolfe A. M., Broderick J. J., Johnston K. J., Condon J. J., 1978, ApJ, 222, 752
- Wolfe A. M., Davis M. M., 1979, AJ, 84, 699
- Wolfe A. M., Gawiser E., Prochaska J. X., 2003, ApJ, 593, 235
- Wolfe A. M., Gawiser E., Prochaska J. X., 2005, ARA&A, 43, 861
- Wolfe A. M., Turnshek D. A., Smith H. E., Cohen R. D., 1986, ApJS, 61, 249
- York B. A., Kanekar N., Ellison S. L., Pettini M., 2007, MNRAS, 382, L53